# A comparison between high-resolution satellite precipitation estimates and gauge measured data: case study of Gorganrood basin, Iran

Donya Dezfooli, Banafsheh Abdollahi, Seyed-Mohammad Hosseini-Moghari and Kumars Ebrahimi

## ABSTRACT

The aim of this paper is to evaluate the accuracy of the precipitation data gathered from satellites including PERSIANN, TRMM-3B42V7, TRMM-3B42RTV7, and CMORPH, over Gorganrood basin, Iran. The data collected from these satellites (2003–2007) were then compared with precipitation gauge observations at six stations, namely, Tamar, Ramiyan, Bahlakeh-Dashli, Sadegorgan, Fazel-Abad, and Ghaffar-Haji. To compare these two groups, mean absolute error (MAE), bias, root mean square error (RMSE), and Pearson correlation coefficient criteria were calculated on daily, monthly, and seasonal basis. Furthermore, probability of detection (POD), false alarm ratio (FAR), and critical success index (CSI) were calculated for these datasets. Results indicate that, on a monthly scale, the highest correlation between observed and satellite-gathered data calculated is 0.404 for TRMM-3B42 at Bahlakeh-Dashli station. At a seasonal scale, the highest correlation is calculated for winter data and using PERSIANN data, while for the other seasons, TRMM-3B42 data showed the best correlation with observed data. The high values of RMSE and MAE for winter data showed that the satellites provided poor estimations at this season. The best and the worst values of RMSE for studied satellites belonged to Sadegorgan and Ramiyan stations, respectively. Furthermore, the PERSIANN gains a better CSI and POD while TRMM-3B42V7 showed a better FAR.

**Key words** | CMORPH, daily precipitation, PERSIANN, remote sensing, statistical evaluation, TRMM

**Donya Dezfooli**
**Banafsheh Abdollahi**
**Seyed-Mohammad Hosseini-Moghari**
**Kumars Ebrahimi** (corresponding author)
Department of Irrigation & Reclamation Engineering,
University of Tehran,
Karaj,
Iran
E-mail: *ebrahimik@ut.ac.ir*

## INTRODUCTION

Global precipitation observations are of paramount importance in climate studies and examination of hydrological models. Therefore, accurate precipitation measurement at global and local scales plays a crucial rule in a better understanding of the climate, hydrological cycle, simulation of hydrological processes and weather forecasts (Qin *et al.* 2014; Cai *et al.* 2015; Milewski *et al.* 2015). Given the fact that rain gauge stations are scattered and are accessed with substantial delays, it seems necessary to resort to other ways of precipitation estimations (Ghajarnia *et al.* 2015). Over the past three decades, a number of studies have been performed to develop different methods of precipitation measurements through making use of satellite images in order to improve the accuracy and make precipitation estimates in regions that lack comprehensive and reliable data (Liu *et al.* 2015).

The only direct source of precipitation measurement is rain gauges, which might sometimes lack accuracy due to various reasons, including errors made by users, device failure, and sensitivity and the impossibility of installing recorders in impassable regions. Furthermore, due to limitations in the number of rain gauge stations, no proper spatial distribution could be envisaged for precipitation. Providing an overhead spatial coverage, satellites are nowadays

doi: 10.2166/aqua.2018.062

capable of making precipitation estimates for the entire world. Thanks to such developments, access has been provided to precipitation data, especially in developing countries such as Iran in which there are no reliable precipitation data in many areas (Moazami *et al.* 2016).

Evaluations of precipitation data provided by satellites have been used in many areas, including drought studies (Zargar *et al.* 2011; Zeng *et al.* 2012; Aghakouchak *et al.* 2015; Sahoo *et al.* 2015; Toté *et al.* 2015), humidity forecast (Gupta *et al.* 2014), and flood (Curtis *et al.* 2007; Nguyen *et al.* 2015; Shah & Mishra 2016) and in rainfall–runoff modeling (Hong *et al.* 2006; Meskele & Moradkhani 2009; Behrangi *et al.* 2014; Falck *et al.* 2015; Sun *et al.* 2015; Toté *et al.* 2015; Zubieta *et al.* 2015).

Making use of satellite images, various methods have been developed that rely on precipitation estimate algorithms including Precipitation Estimation from Remotely Sensed Information using Artificial Neural Networks (PERSIANN; Sorooshian *et al.* 2000; Hsu *et al.* 2012), Climate Prediction Center (CPC), Morphing technique product (CMORPH; Joyce *et al.* 2004), Tropical Rainfall Measuring Mission (TRMM), and Multi-sensor Precipitation Analysis (TMPA) (Huffman *et al.* 2007). The evaluation of satellite rainfall estimates accuracy in comparison to precipitation observation gauge has been carried out in different spatial and temporal resolutions over several regions and basins of the world (Cohen Liechti *et al.* 2012; Kizza *et al.* 2012; Chen *et al.* 2013; Gao & Liu 2013; Xue *et al.* 2013; Conti *et al.* 2014).

Prior to any operational use, it is required to compare the satellite precipitation data with rain gauge observations, ensure their accuracy, and correct them to the extent possible. Several studies have been done in this regard across the world.

Hong *et al.* (2007) analyzed PERSIANN dataset in the northwest of Mexico and showed that it provides reasonable temporal–spatial precipitation estimation in the region under study. Ebert *et al.* (2007) concluded that the data provided by CMORPH show the best daily precipitation probability of detection (POD) in England and Australia. Jiang *et al.* (2012) compared precipitation data provided by CMORPH, TMPA-3B42V6, and TMPA-3B42RT with rain gauges in the southern part of China. They reported that TMPA-3B42V6 showed the best conformity with the rain gauges' observation. Qin *et al.* (2014) analyzed precipitation data provided by TRMM-3B42, TRMM-3B42RT, CMORPH, and GSMaP1 in China. TRMM-3B42 provided the best estimation regarding precipitation data at observation stations. Yuan *et al.* (2017) compared streamflow simulation with TRMM-3B42 and Global Precipitation Measurement (GPM) in Myanmar and reported the superiority of TRMM-3B42. According to Katiraie-Boroujerdy *et al.* (2017), for evaluation of PERSIANN-CDR data and TRMM-3B42V7 with an *in-situ* rain gauge, TRMM-3B42 and PERSSIAN-CDR, respectively, tend to overestimate and underestimate the results. Both satellite products show better correction and RMSEs for the annual mean of consecutive dry periods in comparison to the wet periods. Hobouchian *et al.* (2017) evaluated the accuracy of TRMM-3B42V7, TRMM-3B42RT, CMORPH, and Hydro-Estimator (HYDRO) over the slopes of the subtropical Andes. Their study revealed that errors decrease in winter. Moreover, all satellite data underestimated the precipitation during their analyzed period. Tan & Duan (2017) compared the performance of GPM with TRMM over Singapore at daily, monthly, seasonal, and annual scales. They showed that the monthly results outperform other time scales and, overall, GPM revealed slightly better performance in comparison with other measurements.

Given the importance of precipitation data as primary data in many studies on water resources and lack of an accumulated rain gauge network in many regions of developing countries, impassable ones in particular, it seems necessary to make further use of satellite data to estimate precipitation in various regions. Therefore, scientists have made an effort to assess the accuracy of the data at various spatial and temporal scales. Three large-scale studies have been conducted to assess the accuracy of satellite-driven precipitation in Iran. Moazami *et al.* (2013) studied the accuracy of the data provided by PERSIANN and TRMM-3B42V7 on 47 precipitation events that occurred in winter and spring in Iran over the years 2003 to 2006. Moazami *et al.* (2016) conducted another regional study on four datasets, namely, PERSIANN, CMORPH, TRMM-3B42RT V7, and TRMM-3B42V7 at a daily scale. Since these studies were conducted at different times, the obtained results for the same region were different, suggesting the significance of different time scales in precipitation estimations. In addition, Darand

et al. (2017) studied TMPA at daily and monthly scales in Iran over the years 1998 to 2013. However, there are three points missing in previous studies: (1) datasets' performance at smaller scales, such as basins, is of paramount importance, (2) the analysis of performance variability of datasets at smaller spatial scale and inter-basin, and (3) the assessment of datasets at monthly and seasonal scales, which could be of great assistance in drought studies. The present study aims to assess the reliability and accuracy of the daily, monthly, and seasonal precipitation data provided by PERSIANN, TRMM-3B42V7, TRMM-3B42RT V7, and CMORPH over the Gorganrood basin located in the northeast of Iran. To the best of our knowledge, there is not any record of study regarding this issue in the literature. Steps involved in the present study are as follows.

## MATERIALS AND METHODS

### Case study

Occupying an area of 11,380 $km^2$, Gorganrood basin is located in the northeast of Iran and southeast of the Caspian Sea. It stretches from north to the basin of Lower Atrak, from south to the basins of the Salt Desert, from west to the Caspian Sea, and from southwest to Neka River basin. Alborz heights encompass the southern and eastern parts of the basin. Regarding the geographical location, it is located between the latitudes of 36° 33′ and 37° 45′N and longitudes of 54° 03′ and 56° 13′E. Its highest and lowest altitudes are approximately 600 and 26 meters above sea level, respectively. The annual mean precipitation at Gorganrood basin varies from 300 mm in the northern and southern parts to 1,000 mm in its central part. The maximum precipitation is in the lower regions in the fall as well as the high altitude regions and the regions far from the bank in the winter. The annual mean temperature ranges from 18 °C at low altitude regions to 7.5 °C in southern heights. The annual mean evaporation changes from 1,000 mm at the bank to over 2,000 mm in high altitude regions and the regions far from the bank (non-coastal areas). The Gorganrood watershed consists of many small and large rivers, which together form two main rivers named Gorganrood and Gharehsoo. Running east to west, they flow into the Caspian Sea. The basin's rivers have a rainfall–snow regime and a considerable amount of their annual discharge occurs in non-agricultural seasons, spring flood, and summer flood in some years. The present study made use of daily precipitation data collected from the six stations of Tamar, Ramiyan, Bahlakeh-Dashli, Sadegorgan, Fazel-Abad, and Ghaffar-Haji over the years 2003–2007. Table 1 shows the properties of these stations while Figure 1 depicts their geographical locations.

### PERSIANN

PERSIANN is a precipitation estimation algorithm that employs remote sensing information through an artificial neural network. It has been developed to estimate rainfall at a resolution of $0.25° \times 0.25°$ (Sorooshian *et al.* 2000). Its approach is to calibrate infrared (IR) data through estimation of passive microwave (PMW). It performs by updating parameters at any time that PMW estimations are available. Estimations are made by IR waves and then calibrated by PMW. The algorithms of PERSIANN retrieve precipitation data from satellites, obtain data from visible to

**Table 1** | Details regarding the utilized rain gauge stations of the basin

| Station | Type | Longitude | Latitude | Elevation (m) | Average annual precipition (mm) | Average annual temperature (°C) |
|---|---|---|---|---|---|---|
| Tamar | Evaporation station | 55° 56′ | 37° 56′ | 132 | 537 | 17.9 |
| Ramiyan | Rain gauge | 55° 08′ | 37° 01′ | 200 | 858 | 16.6 |
| Bahlakeh-Dashli | Evaporation station | 54° 47′ | 37° 04′ | 24 | 392 | 17.2 |
| Sadegorgan | Evaporation station | 54° 46′ | 37° 12′ | 12 | 332 | 18.1 |
| Fazel-Abad | Rain gauge | 54° 45′ | 37° 12′ | −22 | 435 | 17.5 |
| Ghaffar-Haji | Evaporation station | 54° 08′ | 37° 00′ | 210 | 674 | 17.2 |

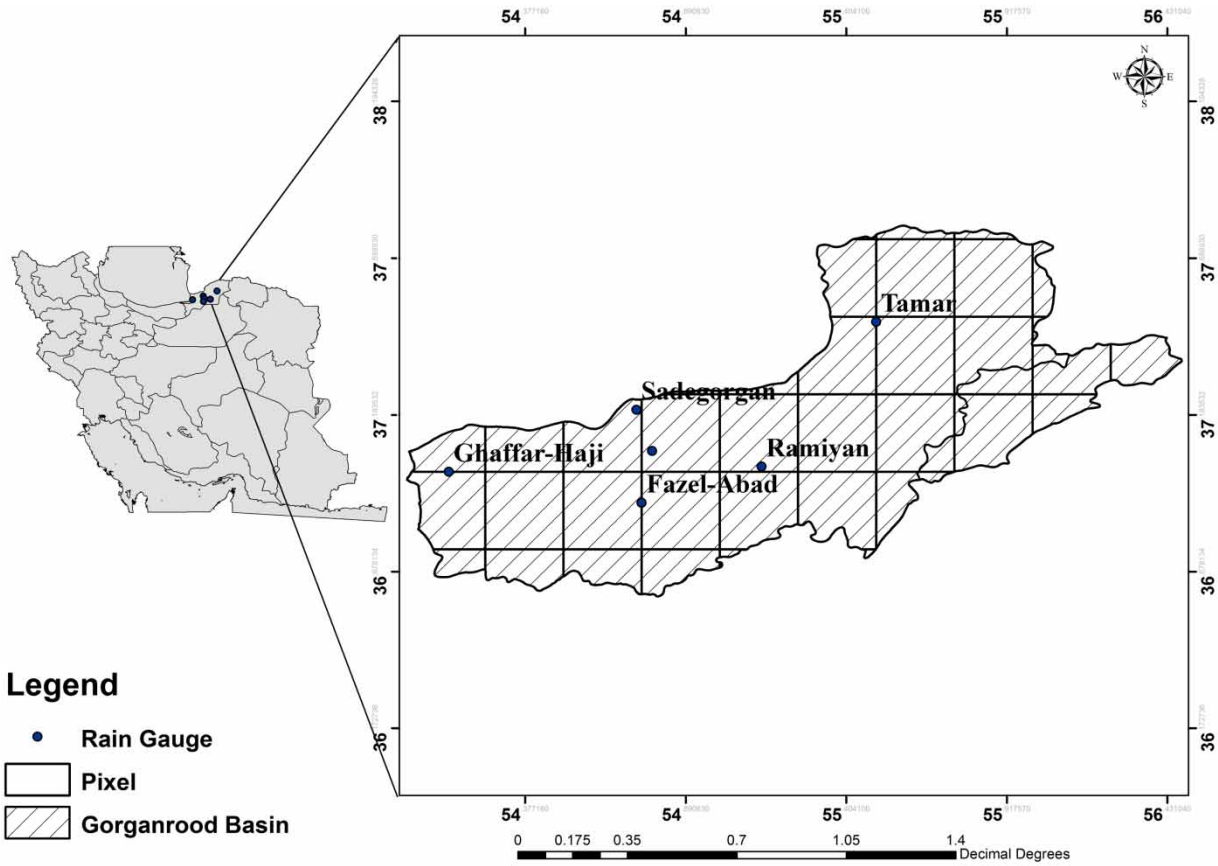


**Figure 1** | Grid reference of satellite data along with the location of the utilized rain gauge stations.

IR images from Geostationary Earth Orbital (GEO) satellites, and extract PMW images from Low Earth Orbital (LEO) satellites (Hsu *et al.* 2012). Its parameters are regularly updated by low-orbital satellite images including F15, F14, DMSP F13, NOAA-16, NOAA-15, and TRMM. Making use of this method, it is possible to recursively perform calibration conformity in different regions (Hsu & Sorooshian 2009; Ghajarnia *et al.* 2015). Relying primarily on IR wave information, and used since 1979, PERSIANN has properly estimated historical precipitation over the past three decades (Ashouri *et al.* 2015). The data are available at http://chrsdata.eng.uci.edu/.

### TRMM-3B42/3B42RT V7

TRMM satellite was designed on 27 November 1997 for a joint space mission between National Aeronautics and Space Administration (NASA) and Japanese Aerospace Exploration Agency (JAXA). Its mission was to estimate precipitation in tropical areas, which constitutes a significant part of precipitation on Earth (Simpson *et al.* 1988). It enjoys a $0.25^\circ \times 0.25^\circ$ spatial resolution and a 3-hourly temporal resolution (Huffman & Bolvin 2015; Kenabatho *et al.* 2017). A couple of versions of data have been produced so far since launching this satellite. The present paper makes use of TRMM-3B42V7 and TRMM-3B42RT V7 products. These products are generated in four phases: (1) the precipitation estimations made by microwave are combined and calibrated; (2) the calibrated microwave precipitation is used to create IR precipitation estimations; (3) IR and microwave estimations are put together; and (4) the data are rescaled to a monthly basis (Huffman *et al.* 2007; Huffman & Bolvin 2015). RT is a near-real version of TRMM-3B42. The difference between these two versions is that the data provided by TRMM-3B42 are corrected by rain gauge observations while no correction is made in data provided by

TRMM-3B42RT (Qin *et al.* 2014). The data are available on the NASA website at https://pmm.nasa.gov/data-access/downloads/trmm.

### CMORPH

CMORPH was introduced by Joyce *et al.* (2004) in the NOAA climate prediction center. The output of CMORPH is the precipitation volume based on satellite images. It has been available on the NOAA website (ftp://ftp.cpc.ncep.noaa.gov/precip/) since December 2002. LEO-based PMW data from different sources, such as TRMM, F-13, F-14, F-15, and F-16, are used by CMORPH to estimate the relevant rain rate with the help of a morphing method. Moreover, infrared data retrieved from geostationary satellites are used to estimate the cloud systems motion with propagation vectors (Ashouri *et al.* 2015; Land Information System 7.1 Reference Manual 2015). The data provided are accessible at a spatial resolution of 0.07° ($8 \times 8\ m^2$), $0.25° \times 25°$, and temporal resolution of 30 minutes, 3 hourly, and daily. Its latitude coverage is 60S–60N (Habib *et al.* 2012). Table 2 summarizes the specifications of these four datasets.

The present study makes use of two sets of precipitation data, namely, (1) daily observation data collected from studied stations over Gorganrood basin and (2) daily precipitation data gathered from PERSIANN, TRMM-3B42V7, TRMM-3B42RT V7, and CMORPH over the period from September 2003 to September 2007. As mentioned earlier, Figure 1 depicts the locations and the corresponding networks of rain gauge stations.

### Evaluation statistics

Four evaluation statistics, namely, bias, mean absolute error (MAE), root mean square error (RMSE), and Pearson correlation coefficient (PCC) were used to assess the reliability of precipitation data provided by the above-mentioned datasets (for more details, see Kottegoda & Rosso (2008)). These criteria are defined as follows:

1. Bias: the mean difference between precipitation estimated by datasets and that of observation station. Bias is either positive or negative, which respectively represents overestimation and underestimation of the observed precipitation volume.

$$Bias = \frac{\sum_{i=1}^{N} (P_{S_i} - P_{O_i})}{N} \tag{1}$$

2. MAE: the mean magnitude of the errors.

$$MAE = \frac{\sum_{i=1}^{N} |P_{S_i} - P_{O_i}|}{N} \tag{2}$$

3. RMSE: measures the mean magnitude of the errors; the higher the RMSE the greater the error.

$$RMSE = \sqrt{\frac{\sum_{i=1}^{N} (P_{S_i} - P_{O_i})^2}{N}} \tag{3}$$

4. PCC: the mean deviation of two variables from their means divided by their standard deviations. The values range between −1 and 1.

$$PCC = \frac{\sum_{i=1}^{N} (P_{S_i} - \overline{P_S})(P_{O_i} - \overline{P_O})}{\sqrt{\sum_{i=1}^{N} (P_{S_i} - \overline{P_S})^2} \sqrt{\sum_{i=1}^{N} (P_{O_i} - \overline{P_O})^2}} \tag{4}$$

where $P_{S_i}$ is the precipitation estimated by datasets on the ith day, $P_{O_i}$ is the observed precipitation volume on the ith

**Table 2** | Summarized estimates of four precipitation satellites including PERSIANN, CMORPH, TRMM-3B42V7, and TRMM-3B42RT V7

| Name | Temporal resolution | Space resolution | Domain | Corrected by gauges | Period | Reference |
|---|---|---|---|---|---|---|
| PERSIANN | 0.5 hr | 0.25° | 60N ~ 60S | No | 2000–present | Ashouri *et al.* (2015) |
| TRMM-3B42 | 3 hr | 0.25° | 50N ~ 50S | Yes | 1998–present | Huffman & Bolvin (2015) |
| TRMM-3B42RT | 3 hr | 0.25° | 50N ~ 50S | No | 1998–present | Huffman & Bolvin (2015) |
| CMORPH | 0.5 hr | ~0.07° | 60N ~ 60S | No | 2002–present | Joyce *et al.* (2004) |

day, N is the daily occurrence of precipitation, $\overline{P_S}$ is the mean precipitation estimated by datasets for N occurrence of daily precipitation in any pixel, and $\overline{P_O}$ is the mean precipitation volume at observation stations for N occurrence of daily precipitation.

Statistics classification indexes including POD, FAR, and CSI are used in the present study to evaluate the precipitation estimations made by datasets under study.

POD shows the ratio of the correct detection of datasets' precipitation to the overall occurrence of precipitation at observation stations.

$$POD = \frac{a}{a+c} \tag{5}$$

FAR shows the cases in which precipitation has been predicted by datasets while no precipitation occurred at the observation stations.

$$FAR = \frac{b}{a+b} \tag{6}$$

CSI shows the ratio of the correct precipitation by datasets.

$$CSI = \frac{a}{a+b+c} \tag{7}$$

where $a$ represents the number of correct predictions of precipitation made by datasets, $b$ represents the number of occurrences in which the precipitation is predicted by datasets while no precipitation occurs at observation stations, and $c$ represents the number of incorrect prediction of precipitation made by datasets. At the best case possible, the values of POD, FAR, and CSI are 1, 0, and 1, respectively.

## RESULTS

The present study compared the precipitation estimated by PERSIANN, TRMM-3B42V7, TRMM-3B42RT V7, and CMORPH datasets to those observed at the following rain gauge stations, namely Tamar, Ramiyan, Bahlakeh-Dashli, Sadegorgan, Fazel-Abad, and Gaffar-Haji over the Gorganrood basin located in Iran. The evaluation was made over the period from September 2003 to September 2007 and the impact of seasonal changes was taken into account.

Figure 2 shows the comparison made at a monthly scale between the precipitation estimation data provided by these four datasets and the observed precipitation at Tamar, Ramiyan, Bahlakeh-Dashli, Sadegorgan, Fazel-Abad, and Ghaffar-Haji stations over the studied period. As Figure 2 illustrates, all four datasets in contrast with the observed data, indicate the same locations for maximum and minimum precipitations. It can be said that the behavior of all four time series at monthly scale resembles the observation data; and in many cases, the increase and decrease in the observed precipitations are consistent with the precipitation estimated by satellites. Moreover, TRMM-3B42V7 shows the best conformity with the observation data over Gorganrood basin, followed by CMORPH, TRMM-3B42RT V7, and PERSIANN in the order of their appearance. At this scale, the highest correlation is related to TRMM-3B42V7 at Bahlakeh-Dashli station, which is equal to 0.404, while the lowest correlation is related to TRMM-3B42RT V7 at Tamar station and is equal to 0.145.

Table 3 presents the mean precipitation taken from the daily-observed data and the daily precipitation estimated by four datasets in each month. For all stations, the highest mean precipitation estimated by these four datasets occurred in January, April, July, August, September, October, November, and December and it was less than the mean observed data. In February, the mean precipitations estimated by PERSIANN and TRMM-3B42RT V7 were higher than mean observed data while the mean precipitations measured by CMORPH and TRMM-3B42V7 in this month were less than the mean observed data. Contrary to the estimations made by the other three datasets, the estimation made by PERSIANN in March was also higher than the mean observed precipitation. It is worth noting that the precipitation estimations made by all four datasets in spring, in June and May in particular, were higher than the mean observed data.

Table 4 shows the standard deviation of daily-observed precipitation data and the daily precipitation estimations made by the datasets in each month. The highest and the

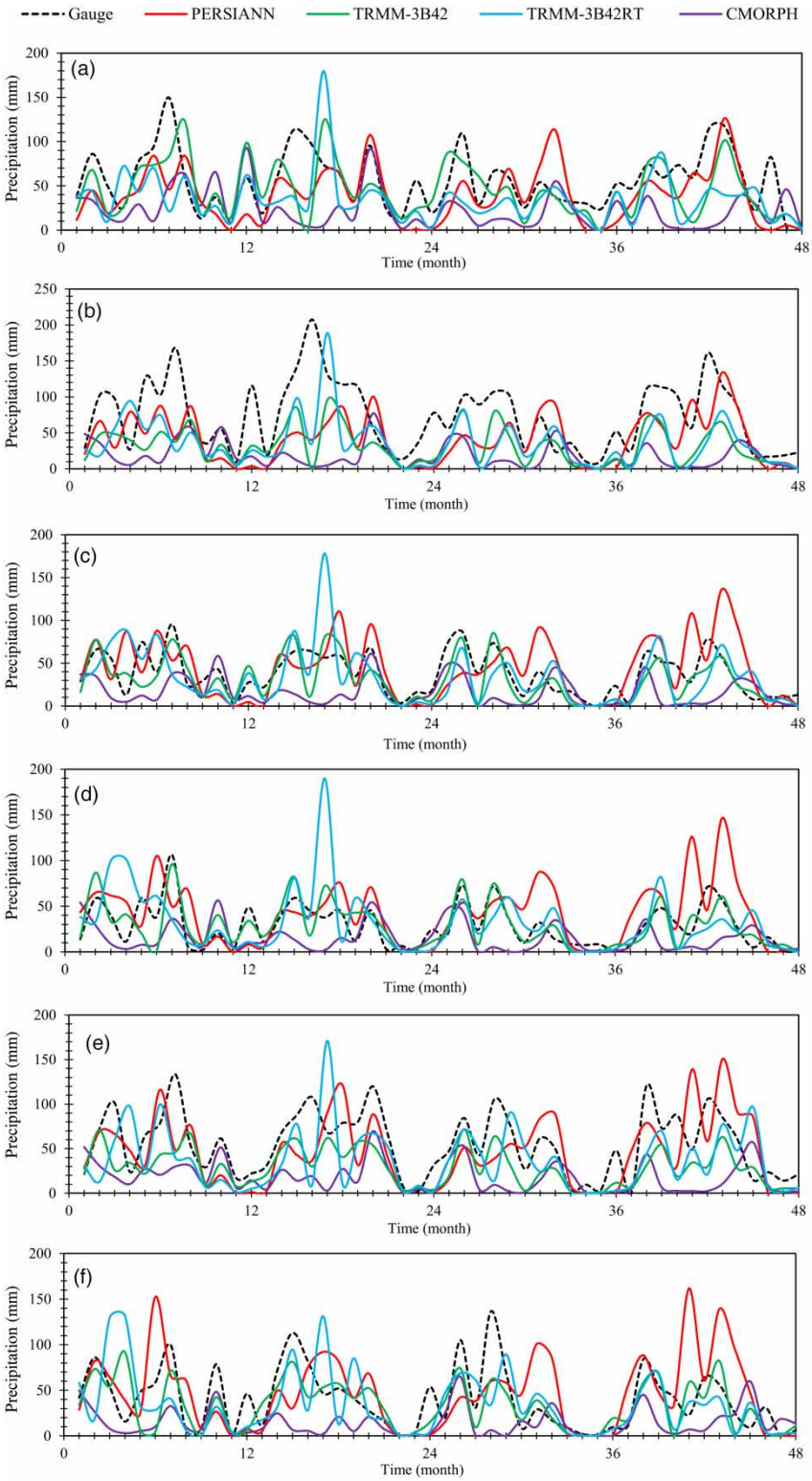


**Figure 2** | Comparison of observed and estimated precipitation of PERSIANN, TRMM-3B42, TRMM-3B42RT, and CMORPH versus each other at monthly scale in Gorganrood basin: (a) Tamar, (b) Ramiyan, (c) Bahlakeh-Dashli, (d) Sadegorgan, (e) Ghaffar-Haji, and (f) Fazel-Abad.

**Table 3** | The mean precipitation for daily-observed data and daily precipitation estimated by four datasets in each month

| | Average | | | | | | | | | | | |
|---|---|---|---|---|---|---|---|---|---|---|---|---|
| | Jan | Feb | Mar | Apr | May | Jun | Jul | Aug | Sep | Oct | Nov | Dec |
| Tamar | | | | | | | | | | | | |
| Observed data | 2.225 | 2.258 | 2.586 | 2.367 | 2.133 | 0.754 | 1.294 | 0.766 | 1.060 | 1.283 | 2.750 | 2.096 |
| PERSIANN | 1.154 | 2.054 | 2.052 | 1.535 | 3.002 | 0.986 | 0.158 | 0.049 | 0.218 | 0.544 | 1.772 | 1.160 |
| TRMM-3B42 | 0.822 | 2.078 | 1.710 | 2.044 | 2.172 | 0.844 | 0.718 | 0.458 | 1.420 | 1.328 | 2.507 | 1.749 |
| TRMM-3B42RT | 1.080 | 2.330 | 1.359 | 1.441 | 1.563 | 1.044 | 0.482 | 0.379 | 0.866 | 0.956 | 1.362 | 1.277 |
| CMORPH | 0.230 | 0.396 | 0.381 | 0.895 | 2.013 | 0.960 | 0.671 | 0.536 | 1.045 | 0.717 | 1.028 | 0.323 |
| Ramiyan | | | | | | | | | | | | |
| Observed data | 1.658 | 1.675 | 1.621 | 1.589 | 1.113 | 0.565 | 0.504 | 0.238 | 0.661 | 1.063 | 2.171 | 1.750 |
| PERSIANN | 1.500 | 2.280 | 2.176 | 1.530 | 2.934 | 0.637 | 0.117 | 0.088 | 0.036 | 0.784 | 1.900 | 1.424 |
| TRMM-3B42 | 1.045 | 1.528 | 1.493 | 1.467 | 1.355 | 0.412 | 0.385 | 0.205 | 0.472 | 0.622 | 2.064 | 1.705 |
| TRMM-3B42RT | 1.308 | 2.588 | 1.365 | 1.624 | 1.695 | 0.699 | 0.334 | 0.154 | 0.430 | 0.696 | 1.461 | 1.943 |
| CMORPH | 0.169 | 0.298 | 0.215 | 0.588 | 1.826 | 0.778 | 0.573 | 0.256 | 0.313 | 0.855 | 1.143 | 0.297 |
| Bahlakeh-Dashli | | | | | | | | | | | | |
| Observed data | 1.658 | 1.675 | 1.621 | 1.589 | 1.113 | 0.565 | 0.504 | 0.238 | 0.661 | 1.063 | 2.171 | 1.750 |
| PERSIANN | 1.696 | 2.306 | 2.471 | 1.708 | 2.613 | 0.754 | 0.114 | 0.113 | 0.041 | 0.816 | 2.116 | 1.589 |
| TRMM-3B42 | 1.180 | 1.377 | 1.322 | 1.524 | 1.158 | 0.449 | 0.316 | 0.222 | 0.495 | 0.560 | 2.043 | 1.455 |
| TRMM-3B42RT | 1.369 | 2.413 | 1.373 | 1.520 | 1.239 | 0.599 | 0.215 | 0.139 | 0.389 | 0.485 | 1.461 | 2.074 |
| CMORPH | 0.171 | 0.166 | 0.211 | 0.532 | 1.380 | 0.712 | 0.591 | 0.168 | 0.237 | 0.795 | 1.183 | 0.232 |
| Sadegorgan | | | | | | | | | | | | |
| Observed data | 1.330 | 1.290 | 1.417 | 1.376 | 0.758 | 0.157 | 0.403 | 0.106 | 0.599 | 0.423 | 1.661 | 1.425 |
| PERSIANN | 1.460 | 2.232 | 2.359 | 1.559 | 2.294 | 0.639 | 0.135 | 0.015 | 0.065 | 0.953 | 1.901 | 1.703 |
| TRMM-3B42 | 1.138 | 1.418 | 0.751 | 1.468 | 0.952 | 0.407 | 0.381 | 0.178 | 0.427 | 0.547 | 1.900 | 1.534 |
| TRMM-3B42RT | 1.530 | 2.697 | 1.133 | 1.331 | 0.961 | 0.586 | 0.270 | 0.075 | 0.132 | 0.655 | 1.135 | 2.363 |
| CMORPH | 0.114 | 0.128 | 0.235 | 0.546 | 1.016 | 0.699 | 0.615 | 0.120 | 0.264 | 0.984 | 1.104 | 0.239 |
| Fazel-Abad | | | | | | | | | | | | |
| Observed data | 2.717 | 2.158 | 2.504 | 2.271 | 2.282 | 0.903 | 0.819 | 0.302 | 0.988 | 0.833 | 2.888 | 2.542 |
| PERSIANN | 1.289 | 2.630 | 2.996 | 1.798 | 2.769 | 1.151 | 0.162 | 0.063 | 0.022 | 0.780 | 2.125 | 1.635 |
| TRMM-3B42 | 1.225 | 1.258 | 1.001 | 1.239 | 1.413 | 0.539 | 0.342 | 0.161 | 0.279 | 0.573 | 1.876 | 1.354 |
| TRMM-3B42RT | 1.140 | 2.817 | 1.567 | 1.307 | 1.568 | 1.264 | 0.190 | 0.101 | 0.126 | 0.743 | 1.343 | 2.119 |
| CMORPH | 0.342 | 0.283 | 0.445 | 0.608 | 1.357 | 0.966 | 0.501 | 0.104 | 0.171 | 0.824 | 1.278 | 0.358 |
| Ghaffar-Haji | | | | | | | | | | | | |
| Observed data | 2.305 | 1.556 | 1.578 | 1.893 | 0.611 | 0.330 | 0.902 | 0.045 | 0.929 | 0.705 | 2.888 | 2.103 |
| PERSIANN | 1.730 | 2.802 | 2.940 | 1.852 | 2.511 | 0.605 | 0.215 | 0.012 | 0.070 | 0.868 | 2.183 | 1.505 |
| TRMM-3B42 | 1.639 | 1.384 | 1.045 | 1.568 | 0.844 | 0.496 | 0.390 | 0.074 | 0.413 | 1.056 | 2.166 | 1.773 |
| TRMM-3B42RT | 1.674 | 2.427 | 0.866 | 1.347 | 0.471 | 0.479 | 0.306 | 0.072 | 0.208 | 1.169 | 1.443 | 2.956 |
| CMORPH | 0.141 | 0.117 | 0.456 | 0.509 | 0.732 | 0.678 | 0.468 | 0.186 | 0.163 | 0.798 | 1.347 | 0.224 |

lowest standard deviations of observed data were seen in November and August, respectively. In general terms, the standard deviation of the observed data was higher than that of the estimated data in all stations, suggesting that the calculated precipitation data have a limited dispersion. The standard deviation of precipitation data estimated by

**Table 4** | The standard deviation of daily-observed precipitation data and the daily precipitation estimations made by the datasets in each month

| | STDEV | | | | | | | | | | | |
|---|---|---|---|---|---|---|---|---|---|---|---|---|
| | **Jan** | **Feb** | **Mar** | **Apr** | **May** | **Jun** | **Jul** | **Aug** | **Sep** | **Oct** | **Nov** | **Dec** |
| Tamar | | | | | | | | | | | | |
| Observed data | 5.357 | 5.611 | 5.631 | 6.146 | 6.993 | 2.085 | 4.036 | 2.945 | 5.046 | 5.486 | 8.043 | 4.915 |
| PERSIANN | 2.492 | 4.410 | 3.880 | 3.502 | 4.909 | 3.956 | 0.848 | 0.231 | 1.082 | 1.681 | 4.288 | 2.533 |
| TRMM-3B42 | 3.459 | 7.396 | 4.852 | 7.006 | 5.716 | 2.622 | 2.005 | 1.533 | 6.656 | 5.448 | 7.358 | 6.399 |
| TRMM-3B42RT | 3.592 | 9.814 | 3.615 | 6.369 | 3.138 | 3.587 | 1.600 | 1.661 | 4.054 | 4.369 | 4.680 | 5.339 |
| CMORPH | 0.965 | 1.717 | 1.200 | 3.909 | 5.298 | 3.482 | 3.366 | 2.753 | 5.336 | 3.045 | 3.296 | 1.002 |
| Ramiyan | | | | | | | | | | | | |
| Observed data | 4.741 | 5.460 | 4.276 | 4.412 | 3.256 | 1.948 | 2.573 | 1.073 | 2.552 | 4.510 | 5.896 | 4.956 |
| PERSIANN | 3.125 | 5.350 | 4.300 | 3.528 | 4.737 | 2.079 | 0.787 | 0.583 | 0.229 | 2.552 | 4.165 | 3.057 |
| TRMM-3B42 | 4.502 | 6.061 | 5.182 | 4.900 | 4.684 | 1.384 | 1.557 | 0.732 | 1.786 | 2.380 | 6.362 | 5.018 |
| TRMM-3B42RT | 4.088 | 9.452 | 3.941 | 5.956 | 4.146 | 2.517 | 1.303 | 0.459 | 1.969 | 3.158 | 5.279 | 5.715 |
| CMORPH | 0.727 | 1.052 | 0.683 | 2.415 | 4.630 | 3.197 | 3.062 | 1.327 | 1.319 | 4.019 | 3.872 | 1.061 |
| Bahlakeh-Dashli | | | | | | | | | | | | |
| Observed data | 4.741 | 5.460 | 4.276 | 4.412 | 3.256 | 1.948 | 2.573 | 1.073 | 2.552 | 4.510 | 5.896 | 4.956 |
| PERSIANN | 3.724 | 5.980 | 4.946 | 3.908 | 4.226 | 2.408 | 0.757 | 1.109 | 0.324 | 3.065 | 4.290 | 3.806 |
| TRMM-3B42 | 4.345 | 5.473 | 4.987 | 5.065 | 3.305 | 1.662 | 1.392 | 1.154 | 2.533 | 2.585 | 6.335 | 4.914 |
| TRMM-3B42RT | 4.540 | 9.838 | 4.067 | 6.248 | 3.422 | 2.740 | 0.864 | 0.706 | 2.420 | 2.858 | 5.141 | 6.357 |
| CMORPH | 0.731 | 0.534 | 0.615 | 2.241 | 3.935 | 3.373 | 3.052 | 0.786 | 1.212 | 3.380 | 4.289 | 1.006 |
| Sadegorgan | | | | | | | | | | | | |
| Observed data | 4.305 | 4.344 | 4.059 | 4.330 | 2.620 | 0.797 | 1.510 | 0.711 | 2.680 | 1.831 | 4.916 | 3.692 |
| PERSIANN | 3.476 | 6.727 | 4.948 | 3.652 | 3.525 | 2.088 | 1.270 | 0.168 | 0.511 | 3.949 | 4.275 | 3.485 |
| TRMM-3B42 | 4.177 | 4.981 | 3.196 | 5.030 | 2.587 | 1.796 | 1.644 | 0.904 | 2.430 | 2.277 | 5.909 | 4.851 |
| TRMM-3B42RT | 5.038 | 9.907 | 3.549 | 5.934 | 2.720 | 2.952 | 1.247 | 0.395 | 0.753 | 3.543 | 3.955 | 7.037 |
| CMORPH | 0.401 | 0.438 | 0.651 | 2.117 | 3.115 | 2.807 | 2.852 | 0.478 | 1.244 | 4.798 | 3.739 | 0.961 |
| Fazel-Abad | | | | | | | | | | | | |
| Observed data | 9.185 | 5.739 | 5.887 | 5.929 | 6.734 | 3.681 | 3.648 | 1.151 | 3.771 | 3.112 | 8.509 | 7.558 |
| PERSIANN | 2.731 | 7.082 | 5.607 | 4.198 | 4.279 | 4.064 | 1.025 | 0.481 | 0.154 | 2.838 | 4.432 | 3.387 |
| TRMM-3B42 | 3.903 | 4.540 | 3.615 | 4.152 | 3.516 | 1.868 | 1.482 | 0.681 | 1.080 | 2.879 | 5.084 | 4.435 |
| TRMM-3B42RT | 4.463 | 10.271 | 4.953 | 5.782 | 3.907 | 5.668 | 0.891 | 0.389 | 0.478 | 3.982 | 4.182 | 5.939 |
| CMORPH | 1.155 | 0.689 | 1.004 | 2.224 | 3.947 | 3.482 | 2.767 | 0.479 | 0.739 | 3.979 | 4.313 | 1.002 |
| Ghaffar-Haji | | | | | | | | | | | | |
| Observed data | 10.215 | 5.525 | 4.344 | 5.867 | 1.697 | 1.386 | 3.887 | 0.298 | 3.577 | 3.679 | 7.561 | 6.352 |
| PERSIANN | 3.976 | 9.180 | 6.340 | 4.359 | 4.477 | 2.418 | 1.573 | 0.115 | 0.601 | 2.815 | 4.531 | 3.375 |
| TRMM-3B42 | 6.323 | 4.375 | 4.275 | 5.041 | 2.846 | 2.822 | 1.946 | 0.473 | 2.138 | 3.794 | 6.399 | 6.765 |
| TRMM-3B42RT | 6.299 | 6.873 | 2.769 | 4.726 | 1.862 | 2.302 | 1.524 | 0.412 | 0.995 | 4.550 | 5.337 | 8.301 |
| CMORPH | 0.556 | 0.439 | 1.279 | 2.025 | 1.951 | 2.321 | 2.555 | 0.733 | 0.608 | 4.416 | 4.878 | 0.942 |

CMORPH in December, January, February, March, and April for all stations was considerably lower than those of the observed data. Furthermore, the calculated values in PERSIANN for standard deviation indicated that compared to other months, the estimated precipitation data in September had less dispersion. In fall, the highest and lowest

standard deviations for all datasets were seen in November and October, respectively.

Table 5 shows the mean values of evaluation criteria at daily and monthly scales. On a monthly scale, all datasets have underestimated at Tamar, Ramiyan, and Fazel-Abad stations. At Bahlakeh-Dashli and Ghaffar-Haji stations, PERSIANN has overestimated while other datasets have underestimated the precipitation data. At Sadegorgan, all datasets except for CMORPH have overestimated the precipitation data.

The correlation coefficient on a daily scale is trivial in the way that the highest and the lowest correlation values of the data provided by PERSIANN with the daily precipitation were 0.244 and 0.106 observed at Sadegorgan and Ramiyan stations, respectively. As for TRMM-3B42V7, the highest and the lowest correlation coefficients were also observed at these two stations at 0.397 and 0.183, respectively. The lowest correlation values on a daily scale were observed in CMORPH and TRMM-3B42RT V7 datasets at Fazel-Abad station at 0.142 and 0.239, respectively. The highest correlation values of these two datasets were seen at Ghaffar-Haji station (0.231) and Bahlakeh-Dashli station (0.366).

As Table 6 illustrates, PERSIANN, TRMM-3B42V7, and TRMM-3B42RT V7 underestimated precipitation data in fall for all stations except Sadegorgan. PERSIANN overestimated in winter at Bahlakeh-Dashli, Sadegorgan, and Ghaffar-Haji stations while it underestimated at Tamar,

**Table 5** | The comparison of the performance criteria for TRMM-3B42RT V7, CMORPH, PERSIANN, and TRMM-3B42V7 based on daily and monthly scales

| Station | Criteria / Scale | PCC | | RMSE | | BIAS | | MAE | |
|---|---|---|---|---|---|---|---|---|---|
| | | Daily | Monthly | Daily | Monthly | Daily | Monthly | Daily | Monthly |
| Tamar | PERSIANN | 0.218 | 0.293 | 5.843 | 5.259 | −0.553 | −0.556 | 2.343 | 2.441 |
| | TRMM-3B42 | 0.287 | 0.307 | 6.487 | 5.712 | −0.340 | −0.344 | 4.186 | 2.458 |
| | TRMM-3B42RT | 0.177 | 0.294 | 6.516 | 5.613 | −0.695 | −0.698 | 1.377 | 2.450 |
| | CMORPH | 0.297 | 0.316 | 5.606 | 5.006 | −1.074 | −1.088 | 1.985 | 1.989 |
| Ramiyan | PERSIANN | 0.106 | 0.221 | 8.732 | 7.611 | −1.062 | −1.069 | 3.183 | 3.201 |
| | TRMM-3B42 | 0.183 | 0.330 | 8.666 | 7.327 | −1.360 | −1.368 | 2.804 | 2.822 |
| | TRMM-3B42RT | 0.145 | 0.286 | 8.928 | 7.530 | −1.229 | −1.239 | 2.956 | 3.210 |
| | CMORPH | 0.243 | 0.334 | 8.263 | 7.027 | −1.789 | −1.809 | 2.450 | 2.463 |
| Bahlakeh-Dashli | PERSIANN | 0.199 | 0.272 | 4.983 | 4.351 | 0.184 | 0.186 | 2.029 | 2.042 |
| | TRMM-3B42 | 0.337 | **0.404** | 4.632 | 3.919 | −0.232 | −0.234 | 1.553 | 1.563 |
| | TRMM-3B42RT | 0.228 | 0.384 | 5.431 | 4.372 | −0.128 | −0.128 | 1.732 | 2.042 |
| | CMORPH | 0.366 | 0.381 | 3.943 | 3.422 | −0.694 | −0.705 | 1.252 | 1.258 |
| Sadegorgan | PERSIANN | 0.244 | 0.344 | 4.472 | 3.701 | 0.417 | 0.420 | 1.722 | 1.733 |
| | TRMM-3B42 | **0.397** | 0.386 | 3.961 | 3.313 | **0.015** | **0.012** | 1.324 | 1.331 |
| | TRMM-3B42RT | 0.210 | 0.381 | 5.116 | 3.955 | 0.126 | 0.128 | 1.523 | 1.730 |
| | CMORPH | 0.315 | 0.387 | **3.490** | **2.968** | −0.419 | −0.427 | **1.080** | **1.084** |
| Fazel-Abad | PERSIANN | 0.199 | 0.313 | 6.492 | 5.653 | −0.308 | −0.307 | 2.481 | 2.495 |
| | TRMM-3B42 | 0.309 | 0.357 | 5.938 | 5.099 | −0.852 | −0.858 | 2.054 | 2.062 |
| | TRMM-3B42RT | 0.142 | 0.287 | 7.203 | 6.133 | −0.603 | −0.605 | 2.422 | 2.528 |
| | CMORPH | 0.239 | 0.319 | 5.968 | 5.118 | −1.211 | -1.222 | 1.922 | 1.929 |
| Ghaffar-Haji | PERSIANN | 0.191 | 0.292 | 6.221 | 5.033 | 0.204 | 0.206 | 2.247 | 2.262 |
| | TRMM-3B42 | 0.328 | 0.362 | 5.656 | 4.657 | −0.214 | −0.217 | 1.810 | 1.821 |
| | TRMM-3B42RT | 0.231 | 0.348 | 6.189 | 4.920 | −0.164 | −0.165 | 1.925 | 2.222 |
| | CMORPH | 0.278 | 0.351 | 5.107 | 3.910 | −0.816 | −0.826 | 1.410 | 1.418 |

**Table 6** | Evaluated criteria for PERSIANN, TRMM-3B42V7, TRMM-3B42RT V7, and CMORPH at seasonal scale

| Season | Station | Dataset | PCC | RMSE | BIAS | MAE | Dataset | PCC | RMSE | BIAS | MAE |
|---|---|---|---|---|---|---|---|---|---|---|---|
| Autumn | Tamar | PERSIANN | **0.353** | 5.813 | −0.884 | 0.147 | TRMM-3B42 | 0.358 | 6.803 | − 0.793 | 0.164 |
| | Ramiyan | | 0.159 | 9.539 | − 1.367 | 0.218 | | 0.311 | 9.096 | −1.390 | 0.189 |
| | Bahlakeh-Dashli | | 0.232 | 5.657 | − **0.154** | 0.151 | | 0.392 | 5.283 | − **0.178** | 0.111 |
| | Sadegoran | | 0.285 | **4.421** | 0.349 | **0.122** | | **0.503** | **3.794** | 0.255 | **0.088** |
| | Fazel-Abad | | 0.347 | 6.593 | −0.574 | 0.165 | | 0.381 | 6.424 | −0.698 | 0.139 |
| | Ghaffar-Haji | | 0.186 | 6.492 | −0.449 | 0.169 | | 0.371 | 6.531 | −0.463 | 0.155 |
| | Tamar | TRMM-3B42RT | 0.283 | 6.862 | −0.822 | 0.153 | CMORPH | **0.432** | 5.771 | −1.329 | 0.123 |
| | Ramiyan | | 0.251 | 9.260 | −1.335 | 0.189 | | 0.317 | 8.923 | −1.935 | 0.160 |
| | Bahlakeh-Dashli | | 0.310 | 5.905 | −0.321 | 0.129 | | 0.399 | 4.675 | −0.905 | 0.092 |
| | Sadegoran | | **0.396** | **4.777** | 0.198 | **0.103** | | 0.398 | **3.724** | − **0.388** | **0.078** |
| | Fazel-Abad | | 0.328 | 6.930 | −0.660 | 0.149 | | 0.385 | 6.250 | −1.242 | 0.124 |
| | Ghaffar-Haji | | 0.304 | 7.153 | − **0.049** | 0.168 | | 0.355 | 5.552 | −1.082 | 0.116 |
| Winter | Tamar | PERSIANN | 0.157 | 6.118 | −0.604 | 0.223 | TRMM-3B42 | 0.109 | 7.201 | −0.793 | 0.194 |
| | Ramiyan | | 0.124 | 11.350 | −1.587 | 0.281 | | 0.007 | 12.130 | −1.864 | 0.269 |
| | Bahlakeh-Dashli | | 0.177 | 6.307 | 0.503 | 0.181 | | 0.173 | 6.141 | **0.170** | 0.142 |
| | Sadegoran | | 0.237 | **5.907** | 0.668 | **0.155** | | 0.150 | **5.315** | 0.313 | **0.122** |
| | Fazel-Abad | | 0.193 | 8.189 | − **0.162** | 0.223 | | 0.272 | 7.132 | −0.432 | 0.168 |
| | Ghaffar-Haji | | **0.256** | 8.582 | 0.491 | 0.199 | | **0.273** | 7.032 | −0.194 | 0.152 |
| | Tamar | TRMM-3B42RT | **0.101** | 7.702 | −0.758 | 0.200 | CMORPH | **0.157** | 5.539 | −1.973 | 0.139 |
| | Ramiyan | | −0.004 | 12.594 | −1.801 | 0.290 | | 0.074 | 11.117 | −3.273 | 0.214 |
| | Bahlakeh-Dashli | | 0.089 | 7.430 | **0.039** | 0.167 | | 0.099 | 4.820 | −1.437 | 0.098 |
| | Sadegoran | | 0.064 | **7.247** | 0.415 | **0.160** | | 0.067 | **4.186** | − **1.159** | **0.080** |
| | Fazel-Abad | | −0.002 | 9.975 | −0.632 | 0.232 | | 0.154 | 7.062 | −2.070 | 0.151 |
| | Ghaffar-Haji | | 0.076 | 8.347 | −0.173 | 0.182 | | 0.058 | 6.460 | −1.548 | 0.112 |
| Spring | Tamar | PERSIANN | 0.171 | 6.793 | 0.161 | 0.204 | TRMM-3B42 | 0.312 | 6.233 | 0.332 | 0.168 |
| | Ramiyan | | 0.041 | 7.601 | 0.219 | 0.221 | | 0.188 | 6.941 | 0.291 | 0.169 |
| | Bahlakeh-Dashli | | **0.261** | 4.491 | 0.770 | 0.145 | | 0.331 | 3.769 | 0.764 | 0.097 |
| | Sadegoran | | 0.208 | **4.450** | 0.957 | **0.134** | | 0.258 | 3.941 | 0.965 | **0.089** |
| | Fazel-Abad | | 0.258 | 6.306 | **0.122** | 0.185 | | 0.266 | 5.667 | **0.091** | 0.153 |
| | Ghaffar-Haji | | 0.199 | 5.067 | 0.498 | 0.155 | | **0.416** | **2.889** | 0.332 | 0.095 |
| | Tamar | TRMM-3B42RT | 0.290 | 5.811 | −0.694 | 0.151 | CMORPH | 0.260 | 6.148 | −0.671 | 0.150 |
| | Ramiyan | | 0.183 | 6.949 | −0.855 | 0.181 | | 0.181 | 6.989 | −1.087 | 0.166 |
| | Bahlakeh-Dashli | | 0.359 | **3.998** | −0.022 | 0.101 | | **0.406** | 3.583 | −0.277 | 0.089 |
| | Sadegoran | | 0.239 | 4.176 | 0.079 | 0.090 | | 0.274 | 3.608 | − **0.080** | 0.079 |
| | Fazel-Abad | | 0.237 | 6.521 | −0.526 | 0.173 | | 0.137 | 6.094 | −1.045 | 0.580 |
| | Ghaffar-Haji | | **0.405** | 4.115 | − **0.017** | **0.086** | | 0.283 | **3.368** | −0.253 | **0.078** |
| Summer | Tamar | PERSIANN | 0.289 | 3.991 | 0.899 | 0.069 | TRMM-3B42 | 0.376 | 4.309 | −0.581 | 0.086 |
| | Ramiyan | | 0.349 | 4.873 | −1.107 | 0.076 | | **0.543** | 4.367 | −0.961 | 0.074 |
| | Bahlakeh-Dashli | | 0.458 | 2.048 | −0.379 | 0.030 | | 0.511 | 2.059 | −0.195 | 0.039 |
| | Sadegoran | | **0.573** | **1.411** | − **0.298** | **0.020** | | 0.525 | **1.662** | −0.136 | **0.032** |

(*continued*)

**Table 6** | continued

| Season | Station | Dataset | PCC | RMSE | BIAS | MAE | Dataset | PCC | RMSE | BIAS | MAE |
|---|---|---|---|---|---|---|---|---|---|---|---|
| | Fazel-Abad | | 0.415 | 2.997 | −0.621 | 0.047 | | 0.382 | 3.062 | −0.533 | 0.054 |
| | Ghaffar-Haji | | 0.464 | 2.571 | −0.548 | 0.039 | | 0.416 | 2.889 | **−0.096** | 0.050 |
| | Tamar | TRMM-3B42RT | 0.333 | 3.903 | −0.462 | 0.079 | CMORPH | 0.310 | 4.346 | −0.301 | 0.083 |
| | Ramiyan | | 0.418 | 4.636 | −0.857 | 0.078 | | 0.506 | 4.356 | −0.789 | 0.071 |
| | Bahlakeh-Dashli | | 0.479 | 2.066 | −0.217 | 0.034 | | **0.561** | **1.823** | **−0.136** | **0.033** |
| | Sadegoran | | **0.505** | **1.579** | **−0.204** | **0.027** | | 0.504 | 1.762 | −0.037 | 0.032 |
| | Fazel-Abad | | 0.360 | 3.076 | −0.549 | 0.050 | | 0.485 | 2.883 | −0.439 | 0.048 |
| | Ghaffar-Haji | | 0.442 | 2.571 | −0.415 | 0.045 | | 0.466 | 2.594 | −0.339 | 0.045 |

Ramiyan, and Fazel-Abad stations. TRMM-3B42RT V7 slightly overestimated at Sadegorgan in the winter. CMORPH and TRMM-3B42V7 underestimated in winter in all stations. While PERSIANN overestimated in all stations except for Ramiyan in spring, TRMM-3B42RT V7 overestimated at Ghaffar-Haji, Bahlakeh-Dashli, and Sadegorgan stations and underestimated at Tamar, Ramiyan, and Fazel-Abad stations. TRMM-3B42V7 overestimated at Sadegorgan and Ghaffar-Haji stations while it underestimated at other stations. CMORPH also underestimated in all stations except Sadegorgan. TRMM-3B42RT V7, TRMM-3B42V7, and CMORPH underestimated in all stations in the summer and PERSIANN also underestimated in all stations except Bahlakeh-Dashli. Generally, it can be said that the highest correlation between the precipitation data collected from the datasets and the observation data was seen in the summer data while the lowest one for all datasets was detected in the winter data. Furthermore, it can be said that PERSIANN shows the best correlation in winter, while in other seasons TRMM-3B42V7 enjoys the best correlation with the observation data.

A comparison of the biases shows that TRMM-3B42V7 and TRMM-3B42RT V7 provided reasonable estimations at Sadegorgan, Bahlakeh-Dashli, and Ghaffar-Haji stations. By comparing the biases obtained from six stations by PERSIANN, it could be inferred that this algorithm often overestimates the precipitation volume in spring, in May in particular, while it underestimates the precipitation in the summer.

RMSE and MAE criteria were used to ensure the accuracy of the estimations. High values of RMSE and MAE in the winter indicate that no reasonable estimation was made by datasets in this season while the lowest values of RMSE and MAE were observed in the summer at the studied stations. Regarding all four datasets, the lowest and highest values of RMSE were detected at Sadegorgan and Ramiyan stations, respectively. In all seasons, the lowest value of MAE was observed at Sadegorgan station. Thus, it could be said that all datasets had a good performance at Sadegorgan station, which is located at a low altitude (12 m), while they could not make proper estimations at Ramiyan station, which is located at a high altitude (200 m). In fact, rainfall estimations are exposed to many factors that may affect precipitation. According to Gottschalck *et al.* (2005), Hong *et al.* (2007), and Romilly & Gebremichael (2011), factors including precipitation volume, seasonal precipitation patterns, precipitation regime, and the region's properties affect the precipitation estimations made by TRMM-3B42, TRMM3B42RT, and PERSIANN datasets. Elevation has an undeniable effect on the precipitation estimation. Hong *et al.* (2007) claimed that the bias of PERSIANN is height-dependent in a way that it underestimates light precipitation at high elevations while it overestimates heavy precipitation at low elevations. For example, PERSIANN in Ghaffar-Haji and Ramiyan stations, which have an elevation of 200 and 210 meters above sea level, respectively, has underestimated light precipitations. In comparison, TRMM at high elevation regions tends to underestimate. On a daily scale, bias values in Tamar are −0.340 and −0.695, in Ramiyan are −1.360 and −1.229, and in Ghaffar-Haji are −0.214 and −0.164 for TRMM-3B42V7 and TRMM-3B42RT V7, respectively. On the contrary, bias values at stations with low elevation such as Bahlakeh-Dashli are −0.232 and −0.128 and in Sadegorgan

are 0.015 and 0.126 for TRMM-3B42 and TRMM3B42RT, respectively. CMORPH in all stations is underestimated but in high elevation stations like Tamar, Ramiyan, and Ghaffar-Haji, as bias on a daily scale is −1.074, −1.789, and −0.816, respectively, the precipitation has been estimated more reliably. Table 6 summarizes evaluation statistics in all six stations for all the seasons studied. The highest values are in bold and the lowest values are underlined in this table.

Three indices of CSI, FAR, and POD were examined to determine the limitations in precipitation detection faced by satellite-based precipitation estimation algorithms. The highest values of CSI and POD at 0.593 and 0.275, respectively, belonged to PERSIANN at Fazel-Abad station while the lowest value of FAR belonged to TRMM-3B42V7 at Sadegorgan station. High values of POD indicate that the datasets have detected rainy days properly while high values of FAR suggest that the number of non-rainy days detected by datasets does not show a reasonable conformity with the number observed at the stations. CSI of approximately 0.3 also reveals that both datasets at the stations under study have been inefficient in differentiating rainy days from non-rainy ones. Figure 3 shows the values of these three indices at studied stations. CMOPRH possesses a POD ranging from 0.42 to 0.57, a FAR from 0.64 to 0.75, and a CSI from 0.21 to 0.25 while TRMM-3B42RT V7 has a POD ranging from 0.27 to 0.33, a FAR ranging from 0.61 to 0.72, and a CSI ranging from 0.17 to 0.21. It can be inferred from Figure 3 that the four studied datasets have a low performance in accurately estimating the number of wet and dry days.

In their analysis of meteorological drought, Sahoo *et al.* (2015) applied information provided by TRMM-3B42V6, TRMM-3B42V7, and TRMM-3B42RT V7 and found that comparing them with other TRMM products TRMM-3B42V7 shows the best performance. These results are consistent with those obtained in the present study. Romilly & Gebremichael (2011) studied the precipitation data over Utopia river basin provided by CMORPH and concluded that precipitations were underestimated in winter while overestimated in summer. However, it was revealed in the present study that both datasets have underestimated precipitations over Gorganrood basin. Cohen Liechti *et al.* (2012) analyzed precipitation data collected from

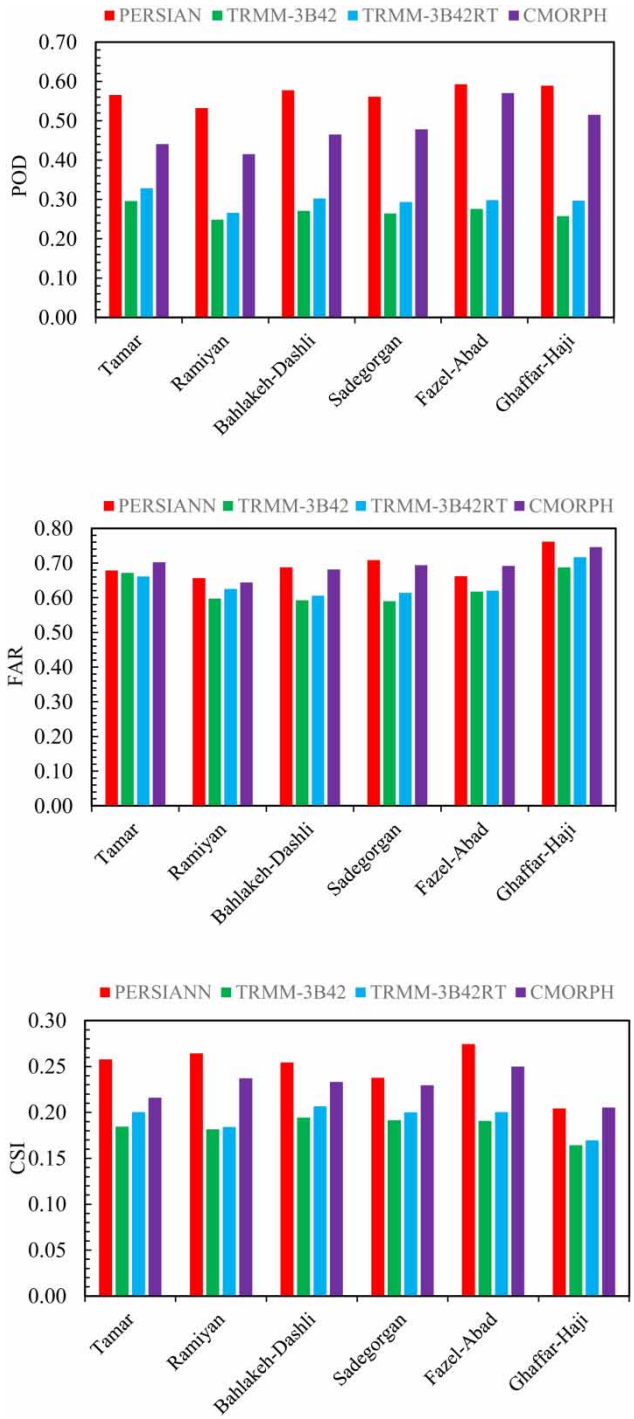


**Figure 3** | Average of POD, FAR, and CSI criteria.

CMORPH and TRMM-3B42 in Africa and concluded that both datasets have overestimated precipitation, compared to observed precipitation. It is contrary to the results

obtained in the present study over the Gorganrood basin. Furthermore, the results revealed that precipitation estimations made through microwaves are generally better than those provided through infrared waves. TRMM-3B42 shows a better conformity with the observation data because of the corrections made at observation stations. It is in line with the results obtained by Gao & Liu (2013), Milewski *et al.* (2015), and Moazami *et al.* (2016).

As mentioned previously, Moazami *et al.* (2013) used 47 precipitation events and concluded that PERSIANN made acceptable precipitation estimations in surrounding areas of the Alborz Mountains. However, Moazami *et al.* (2016) conducted a study on a daily scale on the data provided by four datasets and reported that PERSIANN and TRMM-3B42RT overestimate the precipitation in northern parts of Iran and in the Alborz Mountains. Darand *et al.* (2017) concluded that both TMPA products delivered an appropriate correlation with observation stations in terms of precipitation estimation; however, they tend to underestimate the precipitation in northern parts of Iran. The results obtained from the present study indicated that the variability of datasets' performance occurs on the smaller spatial scale and they deliver various performances in different regions of a basin. Therefore, they should be used more cautiously and assessed specifically for the given area.

It is worth mentioning that performing this research in developing countries always encounters limitations such as the length of time series of data and the number of rain gauges. Moreover, the overall assessment requires further analysis of the datasets' performance based on high-density rain gauge networks relying on long-term statistics that cannot be achieved in the developing countries. However, all available data series used and analyzed for Gorganrood basin in this study were without any gaps. Therefore, this approach is suggested to be evaluated in areas having more *in-situ* data.

## CONCLUSION

Knowledge about the exact precipitation volume plays a crucial role in water resources management. In this regard, due to lack of a spatial distribution of rain gauge stations and delays in access, it is necessary to find proper ways of making precipitation estimations. Making use of satellite-driven data could be considered as one of the most applicable methods in this regard. The present study aimed to assess the accuracy of precipitation data provided by PERSIANN, TRMM-3B42V7, TRMM-3B42RT V7, and CMORPH datasets on daily, monthly, and seasonal scales. Thus, the precipitation data at six stations in the Gorganrood basin were used over a period of 2003–2007. Having analyzed the accuracy of these datasets, it was concluded that TRMM-3B42V7 made the best estimations over Gorganrood basin. Furthermore, estimations made during hot seasons (summer in particular) enjoyed a higher accuracy while estimations made during cold seasons (winter in particular) were not accurate enough. The reason is that the ice existing in the air during cold seasons in low-lying areas is recognized as precipitation by satellites' microwave sensors and thus leads to overestimation of precipitation. The highest correlations belonged to Sadegorgan, Fazel-Abad, and Bahlakeh-Dashli stations, that are located at a lower altitude compared to other stations. The results obtained from daily, monthly, and seasonal analyses showed that the data provided by satellite data on monthly and seasonal scales are more reliable. Hence, it could be concluded that the data provided by satellites could be an alternative to observation precipitations on monthly scales or beyond. Overall, in this study, TRMM-3B42V7 performed better than the other datasets.

## ACKNOWLEDGEMENTS

The authors are very grateful to the University of Tehran for providing all required facilities to do the present study and its papers.

## REFERENCES

AghaKouchak, A., Farahmand, A., Melton, F. S., Teixeira, J., Anderson, M. C., Wardlow, B. D. & Hain, C. R. 2015 Remote sensing of drought: progress, challenges and opportunities. *Reviews of Geophysics* **53** (2), 452–480. doi:10.1002/2014RG000456.

Ashouri, H., Hsu, K. L., Sorooshian, S., Braithwaite, D. K., Knapp, K. R., Cecil, L. D., Nelson, B. R. & Prat, O. P. 2015 PERSIANN-CDR: daily precipitation climate data record

from multisatellite observations for hydrological and climate studies. *Bulletin of the American Meteorological Society* **96** (1), 69–83.

Behrangi, A., Andreadis, K., Fisher, J. B., Turk, F. J., Granger, S., Painter, T. & Das, N. 2014 Satellite-based precipitation estimation and its application for streamflow prediction over mountainous western US basins. *Journal of Applied Meteorology and Climatology* **53** (12), 2823–2842.

Cai, Y., Jin, C., Wang, A., Guan, D., Wu, J., Yuan, F. & Xu, L. 2015 Comprehensive precipitation evaluation of TRMM 3b42 with dense rain gauge networks in a mid-latitude basin, northeast, China. *Theoretical and Applied Climatology* **126** (3–4), 659–671. doi:10.1007/s00704-015-1598-4.

Chen, Y., Ebert, E. E., Walsh, K. J. & Davidson, N. E. 2013 Evaluation of TRMM 3b42 precipitation estimates of tropical cyclone rainfall using PACRAIN data. *Journal of Geophysical Research: Atmospheres* **118** (5), 2184–2196. doi:10.1002/jgrd.50250.

Cohen Liechti, T., Matos, J. P., Boillat, J. L. & Schleiss, A. J. 2012 Comparison and evaluation of satellite derived precipitation products for hydrological modeling of the Zambezi River Basin. *Hydrology and Earth System Sciences* **16** (2), 489–500. doi:10.5194/hess-16-489-2012.

Conti, F. L., Hsu, K. L., Noto, L. V. & Sorooshian, S. 2014 Evaluation and comparison of satellite precipitation estimates with reference to a local area in the Mediterranean Sea. *Atmospheric Research* **138**, 189–204.

Curtis, S., Crawford, T. W. & Lecce, S. A. 2007 A comparison of TRMM to other basin-scale estimates of rainfall during the 1999 Hurricane Floyd flood. *Natural Hazards* **43** (2), 187–198.

Darand, M., Amanollahi, J. & Zandkarimi, S. 2017 Evaluation of the performance of TRMM Multi-satellite Precipitation Analysis (TMPA) estimation over Iran. *Atmospheric Research* **190**, 121–127. doi:10.1016/j.atmosres.2017.02.011.

Ebert, E. E., Janowiak, J. E. & Kidd, C. 2007 Comparison of near-real-time precipitation estimates from satellite observations and numerical models. *Bulletin of the American Meteorological Society* **88** (1), 47–64. doi:10.1175/BAMS-88-1-47.

Falck, A. S., Maggioni, V., Tomasella, J., Vila, D. A. & Diniz, F. L. 2015 Propagation of satellite precipitation uncertainties through a distributed hydrologic model: a case study in the Tocantins–Araguaia basin in Brazil. *Journal of Hydrology* **527**, 943–957.

Gao, Y. C. & Liu, M. F. 2013 Evaluation of high-resolution satellite precipitation products using rain gauge observations over the Tibetan Plateau. *Hydrology and Earth System Sciences* **17** (2), 837–849.

Ghajarnia, N., Liaghat, A. & Arasteh, P. D. 2015 Comparison and evaluation of high resolution precipitation estimation products in Urmia Basin-Iran. *Atmospheric Research* **158**, 50–65. doi:10.1016/j.atmosres.2015.02.010.

Gottschalck, J., Meng, J., Rodell, M. & Houser, P. 2005 Analysis of multiple precipitation products and preliminary assessment of their impact on global land data assimilation system land surface states. *Journal of Hydrometeorology* **6** (5), 573–598.

Gupta, M., Srivastava, P. K., Islam, T. & Ishak, A. M. B. 2014 Evaluation of TRMM rainfall for soil moisture prediction in a subtropical climate. *Environmental Earth Sciences* **71** (10), 4421–4431.

Habib, E., Haile, A. T., Tian, Y. & Joyce, R. J. 2012 Evaluation of the high-resolution CMORPH satellite rainfall product using dense rain gauge observations and radar-based estimates. *Journal of Hydrometeorology* **13** (6), 1784–1798.

Hobouchian, M. P., Salio, P., Skabar, Y. G., Vila, D. & Garreaud, R. 2017 Assessment of satellite precipitation estimates over the slopes of the subtropical Andes. *Atmospheric Research* **190**, 43–54.

Hong, Y., Hsu, K. L., Moradkhani, H. & Sorooshian, S. 2006 Uncertainty quantification of satellite precipitation estimation and Monte Carlo assessment of the error propagation into hydrologic response. *Water Resources Research* **42** (8), 1–15. doi:10.1029/2005WR004398.

Hong, Y., Gochis, D., Cheng, J. T., Hsu, K. L. & Sorooshian, S. 2007 Evaluation of PERSIANN-CCS rainfall measurement using the NAME event rain gauge network. *Journal of Hydrometeorology* **8** (3), 469–482. doi:10.1175/JHM574.1.

Hsu, K. L. & Sorooshian, S. 2009 Satellite-based precipitation measurement using PERSIANN system. In: *Hydrological Modelling and the Water Cycle* (S. Sorooshian, K.-L. Hsu, E. Coppola, B. Tomassetti, M. Verdecchia & G. Visconti, eds). Springer, Berlin, Heidelberg, pp. 27–48.

Hsu, K., Sorooshian, S., Gao, X., Braithwaite, D. & AghaKouchak, A. 2012 Monitoring global precipitation using satellites. *SPIE Newsroom*. doi:10.1117/2.1201210.004475.

Huffman, G. J. & Bolvin, D. T. 2015 *TRMM and Other Data Precipitation Data set Documentation.* NASA, Greenbelt, MD, USA, pp. 1–40.

Huffman, G. J., Adler, R. F., Bolvin, D. T., Gu, G., Nelkin, E. J., Bowman, K. P., Hong, Y., Stocker, E. G. & Wolff, D. B. 2007 The TRMM multi-satellite precipitation analysis (TMPA): quasi-global, multiyear, combined-sensor precipitation estimates at fine scales. *Journal of Hydrometeorology* **8** (1), 38–55. doi:10.1175/JHM560.1.

Jiang, S., Ren, L., Hong, Y., Yong, B., Yang, X., Yuan, F. & Ma, M. 2012 Comprehensive evaluation of multi-satellite precipitation products with a dense rain gauge network and optimally merging their simulated hydrological flows using the Bayesian model averaging method. *Journal of Hydrology* **452**, 213–225.

Joyce, R. J., Janowiak, J. E., Arkin, P. A. & Xie, P. 2004 CMORPH: A method that produces global precipitation estimates from passive microwave and infrared data at high spatial and temporal resolution. *Journal of Hydrometeorology* **5** (3), 487–503.

Katiraie-Boroujerdy, P. S., Asanjan, A. A., Hsu, K. L. & Sorooshian, S. 2017 Intercomparison of PERSIANN-CDR and TRMM-3b42v7 precipitation estimates at monthly and daily time scales. *Atmospheric Research* **193**, 36–49.

Kenabatho, P. K., Parida, B. P. & Moalafhi, D. B. 2017 Evaluation of satellite and simulated rainfall products for hydrological

applications in the Notwane Catchment, Botswana. *Physics and Chemistry of the Earth, Parts A/B/C* **100**, 19–30.

Kizza, M., Westerberg, I., Rodhe, A. & Ntale, H. K. 2012 Estimating areal rainfall over Lake Victoria and its basin using ground-based and satellite data. *Journal of Hydrology* **464**, 401–411. doi:10.1016/j.jhydrol.2012.07.024.

Kottegoda, N. T. & Rosso, R. 2008 *Applied Statistics for Civil and Environmental Engineers*. Blackwell, Malden, MA, USA.

Land Information System 7.1 2015 *Reference Manual*. National Aeronautics and Space Administration, Washington, DC, USA.

Liu, X., Liu, F. M., Wang, X. X., Li, X. D., Fan, Y. Y., Cai, S. X. & Ao, T. Q. 2015 Combining rainfall data from rain gauges and TRMM in hydrological modelling of Laotian data-sparse basins. *Applied Water Science*. **7** (3), 1487–1496. doi:10.1007/s13201-015-0330-y.

Meskele, T. & Moradkhani, H. 2009 Impacts of different rainfall estimates on hydrologic simulation and satellite rainfall retrieval error propagation. In: *World Environmental and Water Resources Congress*, Kansas City, MO, USA. doi:10.1061/41036(342)619.

Milewski, A., Elkadiri, R. & Durham, M. 2015 Assessment and comparison of TMPA satellite precipitation products in varying climatic and topographic regimes in Morocco. *Remote Sensing* **7** (5), 5697–5717. doi:10.3390/rs70505697.

Moazami, S., Golian, S., Kavianpour, M. R. & Hong, Y. 2013 Comparison of PERSIANN and V7 TRMM Multi-satellite Precipitation Analysis (TMPA) products with rain gauge data over Iran. *International Journal of Remote Sensing* **34** (22), 8156–8171. doi:10.1080/01431161.2013.833360.

Moazami, S., Golian, S., Hong, Y., Sheng, C. & Kavianpour, M. R. 2016 Comprehensive evaluation of four high-resolution satellite precipitation products over diverse climate conditions in Iran. *Hydrological Sciences Journal* **61**, 420–440. doi:10.1080/02626667.2014.987675.

Nguyen, P., Thorstensen, A., Sorooshian, S., Hsu, K. & AghaKouchak, A. 2015 Flood forecasting and inundation mapping using HiResFlood-UCI and near real-time satellite precipitation data: the 2008 Iowa flood. *Journal of Hydrometeorology* **16** (3), 1171–1183. doi:10.1175/JHM-D-14-0212.1.

Qin, Y., Chen, Z., Shen, Y., Zhang, S. & Shi, R. 2014 Evaluation of satellite rainfall estimates over the Chinese mainland. *Remote Sensing* **6** (11), 11649–11672. doi:10.3390/rs61111649.

Romilly, T. G. & Gebremichael, M. 2011 Evaluation of satellite rainfall estimates over Ethiopian river basins. *Hydrology and Earth System Sciences* **15** (5), 1505–1514.

Sahoo, A. K., Sheffield, J., Pan, M. & Wood, E. F. 2015 Evaluation of the tropical rainfall measuring mission multi-satellite precipitation analysis (TMPA) for assessment of large-scale meteorological drought. *Remote Sensing of Environment* **159**, 181–193. doi:10.1016/j.rse.2014.11.032.

Shah, H. L. & Mishra, V. 2016 Uncertainty and bias in satellite-based precipitation estimates over Indian sub-continental basins: implications for real-time stream flow simulation and flood prediction. *Journal of Hydrometeorology* **17** (2), 615–636. doi:10.1175/JHM-D-15-0115.1.

Simpson, J., Adler, R. F. & North, G. R. 1988 A proposed tropical rainfall measuring mission (TRMM) satellite. *Bulletin of the American Meteorological Society* **69** (3), 278–295.

Sorooshian, S., Hsu, K. L., Gao, X., Gupta, H. V., Imam, B. & Braithwaite, D. 2000 Evaluation of PERSIANN system satellite-based estimates of tropical rainfall. *Bulletin of the American Meteorological Society* **81** (9), 2035–2046.

Sun, W., Ishidaira, H., Bastola, S. & Yu, J. 2015 Estimating daily time series of streamflow using hydrological model calibrated based on satellite observations of river water surface width: toward real world applications. *Environmental Research* **139**, 36–45. doi:10.1016/j.envres.2015.01.002.

Tan, M. L. & Duan, Z. 2017 Assessment of GPM and TRMM precipitation products over Singapore. *Remote Sensing* **9** (7), 720.

Toté, C., Patricio, D., Boogaard, H., van der Wijngaart, R., Tarnavsky, E. & Funk, C. 2015 Evaluation of satellite rainfall estimates for drought and flood monitoring in Mozambique. *Remote Sensing* **7** (2), 1758–1776. doi:10.3390/rs70201758.

Xue, X., Hong, Y., Limaye, A. S., Gourley, J. J., Huffman, G. J., Khan, S. I., Dorji, C. & Chen, S. 2013 Statistical and hydrological evaluation of TRMM-based multi-satellite precipitation analysis over the Wangchu basin of Bhutan: are the latest satellite precipitation products 3b42v7 ready for use in ungauged basins? *Journal of Hydrology* **499**, 91–99. doi:10.1016/j.jhydrol.2013.06.042.

Yuan, F., Zhang, L., Win, K. W. W., Ren, L., Zhao, C., Zhu, Y. & Liu, Y. 2017 Assessment of GPM and TRMM multi-satellite precipitation products in streamflow simulations in a data-sparse mountainous watershed in Myanmar. *Remote Sensing* **9** (3), 302.

Zargar, A., Sadiq, R., Naser, B. & Khan, F. I. 2011 A review of drought indices. *Environmental Reviews* **19**, 333–349. doi:10.1139/a11-013.

Zeng, H., Li, L. & Li, J. 2012 The evaluation of TRMM Multisatellite Precipitation Analysis (TMPA) in drought monitoring in the Lancang River Basin. *Journal of Geographical Sciences* **22** (2), 273–282.

Zubieta, R., Getirana, A., Espinoza, J. C. & Lavado, W. 2015 Impacts of satellite-based precipitation datasets on rainfall–runoff modeling of the western Amazon basin of Peru and Ecuador. *Journal of Hydrology* **528**, 599–612. doi:10.1016/j.jhydrol.2015.06.064.

First received 13 March 2017; accepted in revised form 13 January 2018. Available online 19 February 2018